Simulation of amphiphilic mesophases using dissipative particle dynamics

CCP

Simon Jury,^a Peter Bladon,^a Mike Cates,^a Sujata Krishna,^a† Maarten Hagen,^b Noel Ruddock^b and Patrick Warren^b

- ^a Department of Physics and Astronomy, University of Edinburgh, JCMB King's Buildings, Mayfield Road, Edinburgh, UK EH9 3JZ
- b Unilever Research, Port Sunlight Laboratory, Quarry Road East, Bebington, Wirral, UK L63 3JT

Received 17th December 1998, Accepted 8th February 1999

We study a dense solution of an amphiphilic species using the dissipative particle dynamics (DPD) algorithm, focusing on the smectic mesophase. Since DPD is locally momentum-conserving, it gives at large length scales a faithful representation of the isothermal hydrodynamics of the system. Results are presented for the phase diagram of a minimal amphiphile model, consisting of rigid AB dimers in a solution of C monomers, for the coarsening dynamics of a polydomain smectic phase, and for the formation of a monodomain smectic when shear is applied.

I Introduction

The formation and flow behaviour of lyotropic liquid crystalline phases shows several interesting features. For example, the evolution of a lamellar (smectic) phase, after a temperature quench from an isotropic phase, can show slow dynamics, typically associated with the sluggish motion of topological defects. Very often, one observes a "polydomain" or "powder" mesostructure in which patches of well-ordered liquid crystal have different orientations; this texture may continue to evolve by slow migration of the defects and domain walls that are present. It is well known that even a weak shearing of such a texture can lead to strong changes in the organization of the defects and domains, and that this in turns affects the rheology and transport properties of the material.¹

Various simulation methodologies have been used to address the phase equilibria of amphiphiles, ranging from phenomenological free energy approaches,² through Monte Carlo lattice models³ to first principles molecular dynamics.⁴ However, few of these can be used to study the time evolution of such structures in three dimensions. In particular, a meaningful study of the coarsening or flow of an ordered phase, such as a smectic (which for simplicity we take to be isothermal after an initial fast quench), should respect the presence of hydrodynamic interactions. These interactions have their origin in the conservation of momentum; and in an isotropic fluid they result in the Navier Stokes equation at large length scales.

However, in a liquid crystalline phase the hydrodynamical equations, such as the Leslie–Ericksen equations for smectics,⁵ are extremely complex, even for a single-species thermotropic material. For lyotropic smectics, such as amphiphilic bilayers in solution, the situation is even worse. Although progress has been made solving the hydrodynamic equations perturbatively, for example, to study the dynamic structure factor of a lamellar monodomain,⁶ there has been little progress so far in numerical modelling of smectic hydrodynamics by con-

ventional continuum mechanical schemes (e.g. finite element) as routinely used for Navier Stokes problems.

This impasse can be negotiated in principle by molecular dynamics (MD). Here one simulates Newton's laws at the level of individual molecules; if this is done correctly, in a regime of parameters where the molecules form a smectic, then the hydrodynamics must be correct. However, we know of no MD studies that have yielded meaningful data on the hydrodynamics of bulk smectics, because the method is limited computationally to short time and length scales.

Dissipative particle dynamics 7-10 offers a third way. As applied to a simple fluid (or fluid mixture) it works as follows. Particles with soft repulsive potentials (allowing a long integration time step) are evolved according to an MD algorithm; however, the pairwise forces between these are subject to additional noise and damping terms, obeying a suitable fluctuation-dissipation theorem.⁸ The latter forces conserve momentum, though not energy; they provide in effect a local thermostat. The method has successfully been used to study various problems,11 most recently that of late-stage demixing in fluid mixtures¹². By stringing DPD particles together, one can extend this approach to study the evolution of polymeric systems, such as block copolymers, 13 with full hydrodynamics (although entanglements are not fully represented due to the soft forces acting). For mesophases, an attraction of the technique is that defects, such as domain walls, are included implicitly in the algorithm, whereas these have to be treated as singularities in continuum hydrodynamics. There is a similar advantage to DPD in binary fluids, where topological reconnection of interfaces is, likewise, handled implicitly.

The DPD approach is comparable in its general philosophy to other mesoscopic modelling methods such as lattice gas and lattice Boltzmann models of amphiphiles.¹⁴ At present, the individual strengths and weaknesses of different mesoscopic techniques largely remain to be clarified. Our own work, is, in any case, among the first mesoscale modelling of amphiphilic mesophases with full hydrodynamics in three dimensions.

In this paper we set up (in Section II below) a minimal DPD model of amphiphiles, which we represent as dimerized (AB) DPD particles in a solvent of monomers (C). For simpli-

[†] Present address: Proctor Department of Food Science, University of Leeds, Leeds, UK LS2 9JT

city we take the the A–A, B–B and C–C interactions to be the same (though different from A–B, B–C and A–C). With suitable energy parameters, we find (in Section III) that this minimal model gives a reasonable phase diagram, in fact, one very similar to a wide range of nonionic surfactants such as $\rm C_{12}E_6$ (albeit without a consolution region in the micellar phase). We then study (Section IV) the formation and coarsening of a smectic phase after a temperature quench. In Section V we give results for the formation of a smectic under flow (with an otherwise similar temperature quench) and also study the orientation and reorganization of a large length-scale domain structure, formed without shear, when a shear is subsequently switched on. Section VI gives a brief conclusion.

II Minimal amphiphiles in DPD

Perhaps the simplest model of an amphiphilic species, within DPD, is a dimer. It is not necessarily obvious that this is adequate: for example, in most lattice approaches it is found that to reproduce the phase equilibria of real surfactants (such as members of the nonionic series $C_n E_m$, where C and E represent ethyl and ethoxy groups) a larger entity containing several monomers (for example A₂B₃) is required.³ However, the soft interactions in DPD are intended to reflect some degree of prior coarse graining. Indeed, Groot et al. 13 show that much of the phenomenology of block copolymer mesophases (which in reality is observed only for fairly long chains) already appears in DPD for quite small "molecules" such as A₃B₇. Therefore a minimal, dimer model of amphiphiles in solution is worth exploring. Note that our work concerns only relatively concentrated systems; we do not address the somewhat delicate effects (critical micellization concentration, etc.) that arise at much lower concentrations. It is not clear that the minimal dimer model would give as good a representation of the latter phenomena as it apparently does for mesophase formation.

The next question is how to impose the dimerization constraint. Given the soft forces, a natural idea is to use a soft constraint, such as a harmonic spring. Indeed, we have made some preliminary studies of phase equilibria and dynamics using such a model. However, in the present work we use instead a rigid dimer model: the AB dimer consists of two DPD particles with a bond of fixed length connecting them. This length is chosen as 0.5 in DPD units as defined below. Although somewhat arbitrary this makes the "size" of the dimer comparable to the interaction range which is approximate to a model in which both the solvent and the surfactant are already coarse grained. (Forces of constraint are added so as to maintain the fixed length.) The rigid dimer model avoids a specific difficulty that can otherwise arise in implementing a dimer model on parallel computers, namely that under some conditions (such as extreme flows) a soft constraint could in principle allow the two members of a dimer to become separated by a large distance in space. Because of the domain decomposition techniques used to partition particles among different processors according to their spatial location, it is much better if all interactions are of strictly finite range; a rigid linkage ensures this.

Otherwise, the interactions between all pairs of particles in the system are of the form used by Groot and Warren.⁹ The conservative forces obey

$$\boldsymbol{F}_{ij}^{C} = \begin{cases} a_{ij}(1 - r_{ij})\hat{\boldsymbol{r}}_{ij} & (r_{ij} < 1) \\ 0 & (r_{ij} \ge 1) \end{cases}$$
 (1)

and the damping forces

$$\boldsymbol{F}_{ij}^{D} = -\gamma w^{D}(\boldsymbol{r}_{ij})(\boldsymbol{v}_{ij} \cdot \hat{\boldsymbol{r}}_{ij})\hat{\boldsymbol{r}}_{ij}$$
(2)

where r_{ij} is the relative displacement and v_{ij} the relative veloc-

ity of a pair of particles of species i, j. The damping weight function is $w^D(r) = (1-r)^2$ for r < 1, and 0 for r > 1; the statistics of the random forces then follow from this by fluctuation—dissipation.^{8,9}

A physical time unit can be defined for each temperature by setting the root-mean-square thermal speed to be $\sqrt{3}$ (so the variance of a single cartesian velocity component is always unity). This choice is basically equivalent to keeping the temperature fixed and varying the interaction energy parameters to control the quench depth (see ref. 9); however, in plotting phase diagrams we choose to retain temperature as a variable, at constant interaction parameters. In our study these were $a_{AA} = a_{BB} = a_{CC} = 25$, $a_{AB} = 30$, $a_{AC} = 0$, $a_{BC} = 50$. The overall scale of these is arbitrary; this choice gives phase diagram features lying in a convenient temperature range around $kT \simeq 1$. These choices leave three physical control parameters: the temperature or thermal energy kT, and a composition variable ϕ , which is the ratio of the number of DPD particles present in the form of dimers, $2N_{AB}$, to the total number $N = 2N_{AB} + N_{C}$. In length units equal to the range of the conservative potential [as in eqn. (1)], the overall particle density $\rho = N/v$ was set as 6 throughout this study. A third control parameter, which physically governs the viscosity (or, for a smectic, viscosities) of the fluid, is γ which was chosen as 5.625 throughout. This choice was motivated by efficiency considerations;9 the resulting viscosity (in DPD units) is 3.51. We leave to future work any investigation of how the viscosity influences the flow behaviour examined below.

Below we report results both from workstation runs (N = 6000) and from major runs on a parallel machine (the Cray T3D located at Edinburgh), for which N = 100000. The former were found adequate for getting a reasonably accurate phase diagram, although some finite size effects were detected on moving to the larger machine. Rather than refine the accuracy of the phase diagram, however, we devoted our parallel computing resources to the study of dynamical effects. Periodic boundary conditions were used throughout. Two slightly different integration routines were used: that on serial machines had a Verlet integrator and, in the time units as defined above, the timestep was chosen as 0.05. The parallel code retains a Euler integrator and a timestep of 0.01. This choice gives measured temperatures within 2% of the nominal value set by the fluctuation-dissipation theorem, which offers a good compromise between absolute accuracy and computer time.

III Phase diagram

Our simulated phase diagram is shown pictorially in Fig. 1. Here we have an array of points indicating the observed state of organization at various compositions ϕ and temperatures kT. The state of organization was found by direct visualizations of the configuration such as those shown for five particular parameter sets. For these visualisations, which are based on tail particles, we inject points into a 50³ grid by a Gaussian splatter. An isosurface is then calculated from the grid. These operations were performed using vtk (a tcl/tk based visualisation package, version 1.3). 15

These runs are relatively small, and some finite size effects do remain. For example, in a hexagonal phase, there will be a tendency for the direction of the cylinders to be inclined at a definite angle with respect to the simulation box so as to get a good match between the favoured repeat distance of the two-dimensional hexagonal packing and the periodicity imposed by the simulation. Because a perfect match cannot be achieved (and because a good match is easier to arrange for lamellae than cylinders) there will be some shift in the phase bound-

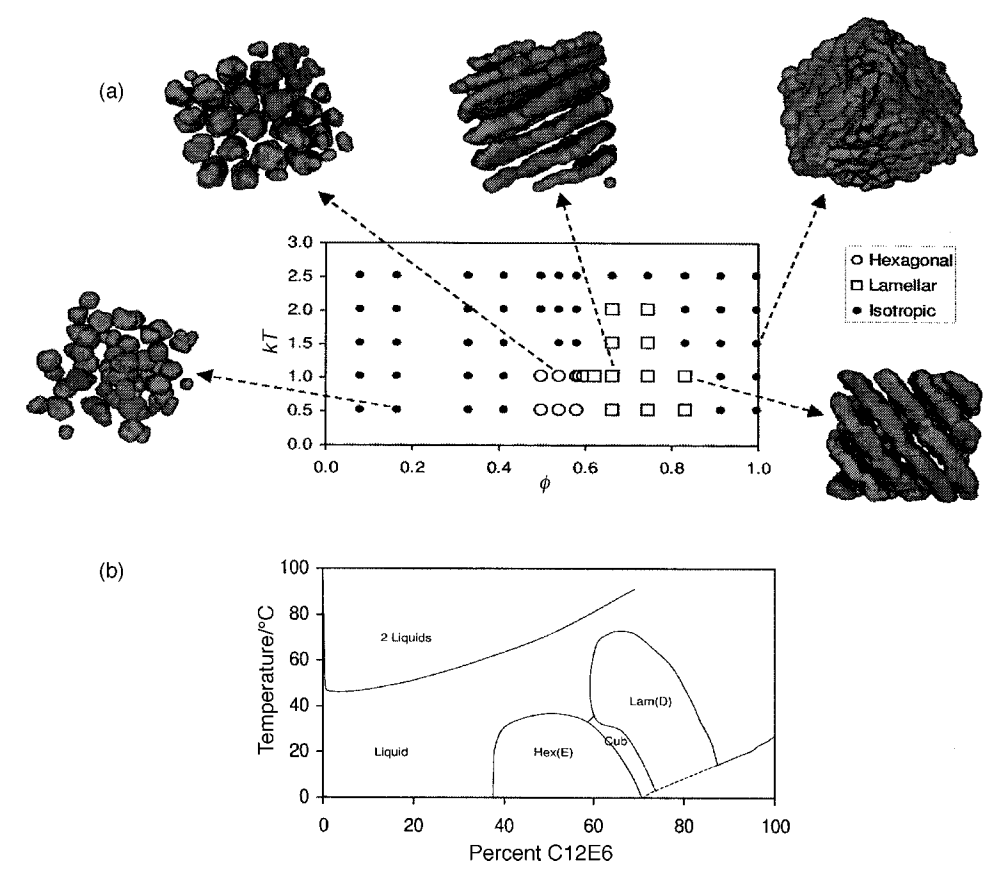


Fig. 1 (a) Top: Phase diagram for DPD dimers. Energy parameters and composition variables are defined in the text. (b) Bottom: Experimental phase diagram for a nonionic surfactant, from ref. 16. Colour representations of these figures are available as supplementary material. Details are available from the Editorial office. For electronic access see http://www.rsc.org/suppdata/cp/1999/2051.

aries on moving to a larger system where the mismatch is less. Also, in a few cases there are signs of trapped defects which make unambiguous phase assignments difficult. Nonetheless, the probable location of the boundaries between isotropic, hexagonal and lamellar phases have been deduced from these simulations. A cubic phase, which should perhaps exist between the hexagonal and the lamellar regions at low kT, was not seen, although we searched quite carefully for one. The resulting phase diagram, Fig. 1(a) may be compared with Fig. 1(b), which shows a classical phase diagram for the nonionic surfactant C₁₂E₆ taken from ref. 16 (see also ref. 17). Given the crudeness of the model, this agreement can be considered reassuring. The main omission is the absence of a two phase region at high temperatures in the low density regime; but since the model has no hydrogen bonding, nor any other attractive forces, this is inevitable. Note that, since we are working with binary systems, the phase boundaries between the various phases should in general be accompanied by miscibility gaps of finite width, for example, we should find a region of ϕ within which lamellar and liquid states coexist. However, it is not surprising that such macroscopic demixing is not observed in simulations of this size, which may not be big enough to contain a well-developed interface between two bulk phases. In any case, for many surfactants, the relevant miscibility gaps are found experimentally to be very narrow; they are not shown at all on many published experimental phase diagrams, including that of Fig. 1(b). This accords with the fact that the various transitions are not strongly first order: there are strong changes in symmetry between the phases, but the difference in local structure either side of the phase boundary is not that great.

IV Formation of lamellar domains after quench

We have studied the dynamic evolution of a quench into a lamellar phase with $\phi = 0.83$, kT = 1.0. The initial condition

was a random arrangement of dimers and monomers. This was done for a system with $N = 100\,000$ on the parallel T3D machine. To monitor the onset of ordering we studied the time evolution of the static structure factor, defined as the Fourier transform of the pair correlator $\langle \rho(r)\rho(0)\rangle - \langle \rho \rangle_2$ where ρ is a suitably chosen combination of local densities n_i . For this study we chose $\rho = n_A + n_B - n_C$; the angle averaged structure factor S(k) is normalized so that $S(k \to \infty) = 1$. Obviously, the precise form of S(k) depends on the particular "contrast" selected, in particular, the relative intensities of the various peaks depends on this.¹⁸ The above choice, in which the contrast is between the solvent (C) and the remainder, gives a large value of the first peak in the structure factor. A slightly different choice, which we also tried, uses the density of dimer *midpoints* to define S(k); in this case the relative intensities of the first and second peaks are almost reversed.

In any case, Fig. 2 shows the time evolution of a strong peak corresponding to the repeat distance of the bilayers (at $k = k_{\text{max}} = 3.2$). By time t = 960 (DPD units) the structure has almost ceased to evolve; a second harmonic (see inset) is by then clearly visible as well. At this stage a further quench was performed to a very low temperature $kT = 10^{-4}$, and the simulation run on for 200 timesteps (20 DPD time units as defined at the pre-quench temperature). This has the effect of dramatically sharpening the interfacial structure, and was done primarily as an aid to visualization. But note that after this final quench one can detect [even in the angle-averaged S(k) three subsidiary peaks at harmonics of the fundamental smectic periodicity. In principle an analysis of the lineshapes of such harmonics could allow determination of the elastic constants of the smectic phase.⁶ However, since the system is not fully equilibrated at its final low temperature ($kT = 10^{-4}$) we do not attempt this here. We do not show angle-resolved data for this system, but we found that the structure factor remains fairly isotropic until quite late times, consistent with the presence of a polydomain texture.

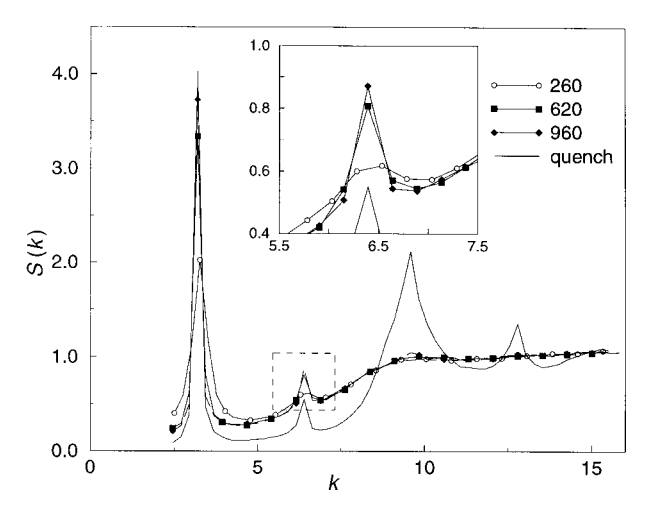


Fig. 2 Time evolution of the angle averaged structure for a quench into the lamellar phase at kT = 1. As the layering increases with time, (t = 260,620,960 DPD units), second and third harmonics develop. A final curve (marked "quench") follows a subsequent quench to $kT = 10^{-4}$.

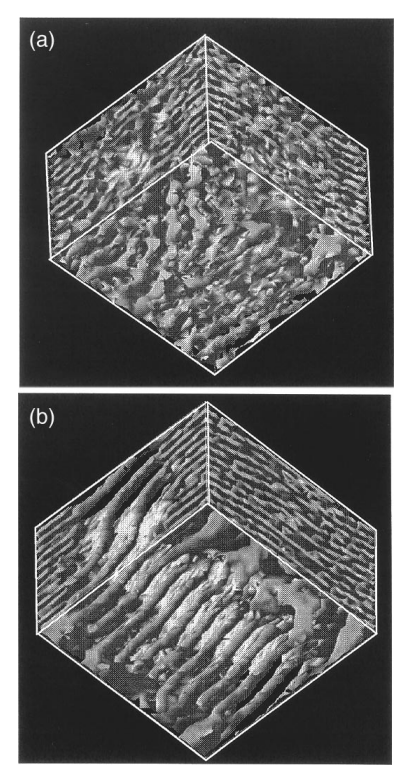


Fig. 3 A quench from random initial particle positions to kT = 1.0in a system with $\phi = 0.83$. (The plotted surface separates head-rich regions from tail-rich and solvent-rich regions; see text for details.) The early time structure (a) has many domains. Late time structure (b) has two. The late time structure has been subjected to a brief further quench to $kT = 10^{-4}$; this is intended to improve the visualisation by sharpening the interfaces. Colour representations of these figures are available, see Fig. 1 for details.

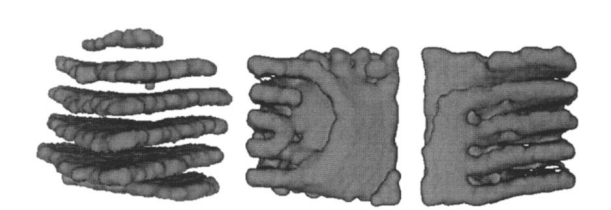


Fig. 4 Features of the bidomain sample: A well-ordered lamellar section and two parts of the domain wall.

For real-space visualizations of these datasets, the interface between media is defined by a zero-set of the density difference $n_{\rm B}-n_{\rm A}-n_{\rm C}$ where the ns represent the local number densities. These are specified on a coarse-grained 32³ grid and the surface plotted using standard interpolation software within the AVS visualisation package. Fig. 3 shows the resulting polydomain texture in real space for a time t = 320 DPD units after the initial quench. This is compared with the same texture after a period of further evolution followed by a final deep quench. Even at the original quench temperature (kT = 1.0) the simulation at this point has almost stopped evolving, it may not be possible for this structure to coarsen further (under periodic boundary conditions) at any significant rate.

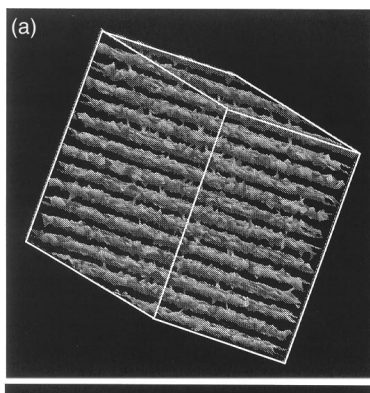
There are now visible just two large smectic domains connected by a topologically nontrivial domain wall. Although it is hard to be certain, we suspect that this structure is already present at the original simulation temperature and that the final quench to $kT = 10^{-4}$ merely serves to sharpen the interfaces. Inspection of the figure shows an apparent density of "necks" (defects connecting one layer to the next) along some but not all of the faces of the simulation cell; these are probably an artefact of the visualization software (which does not respect the periodic boundary conditions), and indeed far fewer necks are seen well within the cell. A cut-out taken from the centre of one of the two large domains is shown in Fig. 4; it shows good smectic ordering with a slight twist (and almost no neck defects). Close-ups of the domain wall structure are also presented there; the visualization method is as in Fig. 1.

Flow effects

Two preliminary investigations of flow effects were made (using the T3D). In the first, we studied the formation of a lamellar mesophase under ambient shearing: a system of volume fraction $\phi = 0.7$ was quenched into the lamellar phase (kT = 1.0), while a steady shear was maintained (using Lees-Edwards boundary conditions). The shear rate was 0.01 in DPD units, which is small compared to the local collision rates for particles but large compared to the relaxation time for a defect texture as shown in Fig. 3. Under these conditions, smectic order was rather quickly achieved, leading to a good monodomain sample by about t = 200 DPD units; see Fig. 5. The layers' normals are perpendicular to the velocity direction (which is unavoidable in a lamellar phase under steady shear) and almost, but not quite, aligned with the velocity gradient. Note that in principle the layer normals could point anywhere on a circle in the velocity gradient/neutral plane, although most theoretical treatments predict one extreme or the other. 19,20

Once a good monodomain was formed, the shearing was then stopped and the structure allowed to relax for a further long period (500 DPD units) before the structure factor for the whole sample was determined. This structure should thus be an equilibrium monodomain (with the proviso that relaxation of the smectic repeat distance may not be possible even in this time period; the mean layer spacing could still be perturbed by the preceding flow). The resulting angle-resolved structure factor is shown in Fig. 5 for the velocity gradient/neutral plane in reciprocal space. (Note that no further quench was needed in this case; kT is still 1.0.) This shows extremely good ordering with four orders of scattering peak; an angle-average of this structure factor (not shown) is very similar to the t = 960 curve shown in Fig. 2. The slight misalignment of the layer normals with the velocity gradient direction is visible in the figure.

In the second T3D run, we investigated the effect of shear on a pre-existing lamellar texture. The bidomain structure already shown in Fig. 3(b) (but at the original quench temperature of kT = 1.0) was subjected to a shear rate of 0.04 in



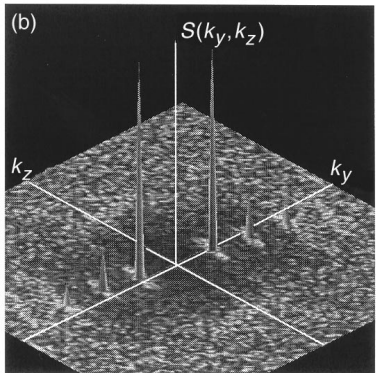


Fig. 5 (a) A monodomain created by shearing the sample from the out-set. (b) Resulting angle-resolved structure factor $S(k_y, k_z)$ with y, z respectively the velocity gradient and neutral directions. Colour representations of these figures are available, see Fig. 1 for details.

DPD units. By t = 200, this too was converted into a well-ordered monodomain sample, very similar to that shown in Fig. 5(a). As before, the layer normals must be perpendicular to the velocity direction; however unlike Fig. 5(a) the layer normals were in this case oriented at roughly 45° midway between the velocity gradient and neutral directions.

It was confirmed, in several smaller workstation runs, that formation of smectic and hexagonal mesophases proceeded rather quickly whenever a relatively small shear rate was maintained after the initial quench. This concurs with widespread experience in the processing of block copolymers, for example in ref. 21. In some cases however, especially at higher shear rates, the structures formed are somewhat perturbed. An example is the "modulated hexagonal phase" seen in Fig. 6. In this run $N = 18\,000$ particles were used in an elongated box, $\phi = 0.54$. The system was sheared for 1000 DPD time units, with a shear rate of 0.05 in DPD units. This type of structure may be an artefact, however: as mentioned before, hexagonal phases, without shear, will tend to align with a specific orientation to the simulation box. If this is incompatible with alignment along the streamlines (the only stable organizations of hexagonal cylinders under shear flow), then frustration may result. The first of these effects is finite-size related, so such modulations might vanish for large system sizes; we have not yet investigated this. Lamellar phases do not have as severe a problem, since the layer spacing can be varied by rotation of the layer normal within in the gradient/neutral plane. Suggestively, we found quite a strong dependence of

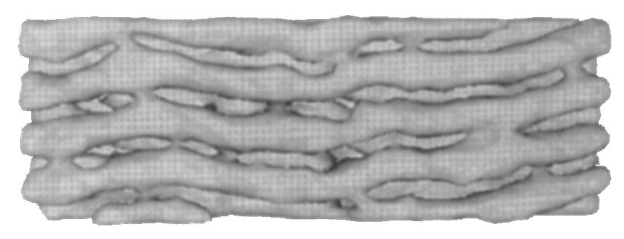


Fig. 6 Hexagonal phase with an undulation, caused by shearing.

lamellar orientation on shear rate at fixed ϕ , so similar physics may be involved here too; however we did not investigate this in detail.

Finally, it is known experimentally that, under sustained steady shear, a lamellar phase can develop an organized texture comprising concentric multilamellar polyhedra (the onion texture) or, in thermotropics, long multilamellar prisms.^{22,23} In practice these arise at very large length scales (micrometres) and therefore cannot really be expected in even the largest simulations performed here. However, we have seen signs of the latter in one or two runs; if confirmed, these will be reported in future work.

VI Conclusions

We have introduced a minimal model of surfactants within the DPD mesoscopic modelling framework. The minimal model comprises rigid dimers, and gives a reasonably good mapping onto the phase equilibria of simple nonionic amphiphiles such as $\rm C_{12}E_6$. The model allows simulations of the coarsening and flow behaviour of smectic mesophases, in three dimensions, with the correct incorporation of hydrodynamic interactions at large distances.

The nature of smectic hydrodynamics is complex⁵ and it might be interesting to test the predictions of the model against theories of linear hydrodynamic fluctuations in smectics, for example the dynamic structure factor.⁶ However, the main value of a model like this is to allow study of nonlinear phenomena, such as the coupling between mesoscale structure and flow fields, which is hard to treat theoretically beyond a few simple cases. In future work we hope to extend our study of the alignment dynamics of smectic domains under shear, begun above, to look at the displacement of the phase boundary (i.e., a shear-induced phase transition¹⁹) between the isotropic and lamellar phases. Future work will also address the introduction of nonminimal amphiphiles which may give a better account of the physics of relatively dilute surfactant solutions and/or ternary mixtures.

Acknowledgements

We thank R. D. Groot and M. Lal for discussions. SIJ thanks Unilever PLC and the EPSRC (UK) for a CASE Award. Work funded in part under EPSRC E7 Grand Challenge.

References

- See, e.g., R. G. Larson and P. T. Mather, in *Theoretical Challenges in the Dynamics of Complex Fluids*, ed. T. C. B. McLeish, NATO ASI Series E, Kluwer, Dordrecht, The Netherlands, 1997, vol. 339.
- G. Gompper and M. Schick, Self-Assembling Amphiphilic Systems, Academic Press, New York, 1994.
- 3 R. G. Larson, J. Phys. II, 1996, **6**, 1441.
- 4 B. Smit, K. Esselink, P. A. J. Hilbers, N. M. van Os and I. Szleifer, *Langmuir*, 1993, 9, 9.
- 5 P. G. de Gennes and J. Prost, The Physics of Liquid Crystals, Clarendon, Oxford, 1993.
- 6 F. Nallet, D. Roux and J. Prost, J. Phys., 1989, 50, 3147.
- 7 P. J. Hoogerbrugge and J. M. V. A. Koelman, Europhys. Lett., 1992, 19, 155.
- 8 P. Español and P. B. Warren, *Europhys. Lett.*, 1995, **30**, 191. Note that the original algorithm of ref. 7 did not implement the fluctuation–dissipation theorem correctly.
- 9 R. D. Groot and P. B. Warren, J. Chem. Phys., 1997, 107, 4423.
- 10 P. B. Warren, Curr. Opin. Colloid Interface Sci., 1998, 3, 620.
- E. S. Boek, P. V. Coveney, H. N. W. Lekkerkerker and P. van der Schoot, *Phys. Rev. E*, 1997, 55, 3124; A. G. Schlijper, P. J. Hoogebrugge and C. W. Manke, *J. Rheol.*, 1995, 39, 567.
- 12 S. I. Jury, P. Bladon, S. Krishna and M. E. Cates, *Phys. Rev. E.*, submitted.
- R. D. Groot and T. J. Madden, J. Chem. Phys., 1998, 108, 875; R. D. Groot, T. J. Madden and D. J. Tildesley, J. Chem. Phys., accepted for publication.

- B. M. Boghosian, P. V. Coveney and A. N. Emerton, Proc. R. Soc. London Ser. A, 1996, 453, 1221; O. Thiessen, G. Gompper and D. M. Kroll, Europhys. Lett., 1998, 42, 419; G. Gonnella, E. Orlandini and J. M. Yeomans, Phys. Rev. Lett., 1997, 78, 1695.
- W. Schroeder, K. Martin and B. Lorensen, The Visualisation Toolkit, Prentice Hall, Englewood Cliffs, NJ, 1996.
- 16 D. J. Mitchell, G. J. T. Tiddy, L. Waring, T. Bostock and M. P. McDonald, J. Chem. Soc., Faraday Trans. 1, 1983, 79, 975.
- 17 R. G. Laughlin, The Aqueous Phase Behavior of Surfactants, Academic Press, New York, 1994.
- 18 If one considers the scattering object to be a bilayer rather than particles then S(k) becomes the product of a structure factor for
- the smectic and a form factor for the bilayer. The latter, though not the former, strongly depends on the contrast chosen.
- 19 M. E. Cates and S. T. Milner, *Phys. Rev. Lett.*, 1989, **62**, 1856.
- 20 C. R. Safinya and R. F. Bruinsma, Phys. Rev. A, 1991, 43, 5377.
- G. H. Fredrickson and F. S. Bates, *Annu. Rev. Mater. Sci.*, 1996, 26, 501.
- 22 O. Diat, D. Roux and F. Nallet, J. Phys. II, 1993, 3, 1427.
- 23 P. Panizza, P. Archambault and D. Roux, J. Phys. II, 1995, 5, 303

Paper 8/09824G